

**[DRAFT] DETC2015-47370**

**MODIFIED BAYESIAN KRIGING FOR NOISY RESPONSE PROBLEMS FOR  
RELIABILITY ANALYSIS**

**Nicholas J. Gaul**

Department of Mechanical & Industrial Engineering  
College of Engineering, The University of Iowa  
Iowa City, IA 52242, USA  
[nicholas-gaul@uiowa.edu](mailto:nicholas-gaul@uiowa.edu)

**Hyunkyoo Cho and K. K. Choi\***

Department of Mechanical & Industrial Engineering  
College of Engineering, The University of Iowa  
Iowa City, IA 52242, USA  
[hyunkyoo-cho@uiowa.edu](mailto:hyunkyoo-cho@uiowa.edu), [kyung-choi@uiowa.edu](mailto:kyung-choi@uiowa.edu)

\*Corresponding author

**Mary Kathryn Cowles**

Department of Statistics & Actuarial Science  
College of Liberal Arts and Sciences, The  
University of Iowa  
Iowa City, IA 52242, USA  
[kate-cowles@uiowa.edu](mailto:kate-cowles@uiowa.edu)

**David Lamb**

US Army RDECOM/TARDEC  
Warren, MI 48397-5000, USA  
[david.lamb@us.army.mil](mailto:david.lamb@us.army.mil)

**ABSTRACT**

This paper develops a new modified Bayesian Kriging (MBKG) surrogate modeling method for problems in which simulation analyses are inherently noisy and thus standard Kriging approaches fail to properly represent the responses. The purpose is to develop a method that can be used to carry out reliability analysis to predict probability of failure. The formulation of the MBKG surrogate modeling method is presented, and the full conditional distributions of the unknown MBKG parameters are presented. Using the full conditional distributions with a Gibbs sampling algorithm, Markov chain Monte Carlo is used to fit the MBKG surrogate model. A sequential sampling method that uses the posterior credible sets for inserting new design of experiment (DoE) sample points is proposed. The sequential sampling method is developed in such a way that the newly added DoE sample points will provide the maximum amount of information possible to the MBKG surrogate model, making it an efficient and effective way to reduce the number of DoE sample points needed. Therefore, the proposed method improves the posterior distribution of the probability of failure efficiently. To demonstrate the developed MBKG and sequential sampling methods, a 2-D mathematical example with added random noise is used. It is shown how, with the use of the sequential sample method, the posterior distribution of the probability of failure converges to capture the true probability of failure. A 3-D multibody dynamics (MBD) engineering block-car example illustrates an application of the

new method to a simple engineering example for which standard Kriging methods fail.

**KEYWORDS**

Bayesian Kriging, Reliability Analysis, Sequential Sampling

**1. INTRODUCTION**

Reliability analysis methods have been developed to analyze the reliability of product designs subject to the randomness of the input variables. Most reliability analysis methods can be classified into one of two groups, the first being sensitivity-based methods and the second being sampling-based methods. The literature is rich with numerous sensitivity-based methods that have been developed using the most probable point [1-6]. Some common sensitivity-based methods are the first-order reliability method (FORM) [5, 7, 8], the second-order reliability method (SORM) [5, 7-9], and the dimension reduction method (DRM) [3, 10, 11]. While these methods can be computationally cheaper than sampling-based methods, one pitfall is that they may not be as accurate as sampling-based methods for highly nonlinear problems [12]. Another shortcoming of these methods is that they require the sensitivity of the performance measures to be available. Obtaining the sensitivity, while possible for some problems, can be a daunting, if not impossible, task for some problems that are highly

## Report Documentation Page

*Form Approved*  
*OMB No. 0704-0188*

Public reporting burden for the collection of information is estimated to average 1 hour per response, including the time for reviewing instructions, searching existing data sources, gathering and maintaining the data needed, and completing and reviewing the collection of information. Send comments regarding this burden estimate or any other aspect of this collection of information, including suggestions for reducing this burden, to Washington Headquarters Services, Directorate for Information Operations and Reports, 1215 Jefferson Davis Highway, Suite 1204, Arlington VA 22202-4302. Respondents should be aware that notwithstanding any other provision of law, no person shall be subject to a penalty for failing to comply with a collection of information if it does not display a currently valid OMB control number.

1. REPORT DATE <b>29 APR 2015</b>	2. REPORT TYPE	3. DATES COVERED <b>00-00-2015 to 00-00-2015</b>			
4. TITLE AND SUBTITLE <b>MODIFIED BAYESIAN KRIGING FOR NOISY RESPONSE PROBLEMS FOR RELIABILITY ANALYSIS</b>		5a. CONTRACT NUMBER			
		5b. GRANT NUMBER			
		5c. PROGRAM ELEMENT NUMBER			
6. AUTHOR(S)		5d. PROJECT NUMBER			
		5e. TASK NUMBER			
		5f. WORK UNIT NUMBER			
7. PERFORMING ORGANIZATION NAME(S) AND ADDRESS(ES) <b>US Army RDECOM-TARDEC,6501 E. 11 Mile Road,Warren,MI,48397-5000</b>		8. PERFORMING ORGANIZATION REPORT NUMBER			
9. SPONSORING/MONITORING AGENCY NAME(S) AND ADDRESS(ES)		10. SPONSOR/MONITOR'S ACRONYM(S)			
		11. SPONSOR/MONITOR'S REPORT NUMBER(S)			
12. DISTRIBUTION/AVAILABILITY STATEMENT <b>Approved for public release; distribution unlimited</b>					
13. SUPPLEMENTARY NOTES					
14. ABSTRACT <b>See Report</b>					
15. SUBJECT TERMS					
16. SECURITY CLASSIFICATION OF:			17. LIMITATION OF ABSTRACT <b>Same as Report (SAR)</b>	18. NUMBER OF PAGES <b>16</b>	19a. NAME OF RESPONSIBLE PERSON
a. REPORT <b>unclassified</b>	b. ABSTRACT <b>unclassified</b>	c. THIS PAGE <b>unclassified</b>			

nonlinear and/or coupled with fluid structure interaction, e.g., crash and blast problems.

To overcome the shortfalls of the sensitivity-based methods, sampling-based methods have been developed. A brute force approach would be to do direct Monte Carlo simulation (MCS) using the computer-aided engineering (CAE) simulation models, e.g., finite element (FE) models and computational fluid dynamic (CFD) models, to calculate the reliability. While this method can be highly accurate using a large number of MCS points [5], its limitation is that it requires very significant computational cost due to a large number of CAE model simulations, thus rendering it impractical. In order to overcome the impractical computational cost of direct MCS using CAE simulations and to overcome the pitfalls of the sensitivity-based methods, the use of surrogate models is becoming a more common practice [13-18]. There are three advantages of using surrogate models. The first is that the sensitivity of the performance measure is not needed to construct the surrogate. The second is that surrogate models are computationally inexpensive to use for evaluating large numbers of MCS points compared to the computational cost of the CAE models. The third is that surrogate models can be built using a limited number of CAE model simulations, therefore reducing the overall computational cost of performing a reliability analysis.

The literature is full of numerous surrogate modeling methods that have been developed over decades and are still being actively developed. The main reason for all the development is that there is not one surrogate modeling method that works for every problem. Some of the common surrogate modeling methods in the literature are, polynomial response surface (PRS) [17, 19-21], polynomial chaos [22], moving least squares (MLS) [19], multivariate adaptive regression splines (MARS) [23], support vector machine and support vector regression [19, 20], virtual support vector machine (VSVM) [24], radial basis functions (RBF) [19, 20, 23], neural networks (NN) [25], ordinary Kriging (OKG) and universal Kriging (UKG) [19, 20, 23, 26, 27], and dynamic Kriging (DKG) [15, 16]. There have been surrogate modeling methods developed that use Bayesian methods [28-31]. However, none of the methods studied claim to do a full Bayesian analysis when creating the surrogate model; they are only borrowing concepts from the Bayesian methods.

As previously described, a surrogate model is used to do the MCS prediction for the reliability analysis for the sampling-based reliability-based design optimization (RBDO) method to ease the computational burden. Thus, the accuracy of the reliability analysis depends on the accuracy of the surrogate model. Kriging has become a popular surrogate modeling method because it offers flexibility in the choice of both the mean structure and the correlation function used [19, 20]. Dynamic Kriging was developed because it was found to be more accurate than OKG or UKG, giving better reliability analysis results [15, 16, 46, 47]. However, OKG, UKG, and DKG are typically formulated and used as interpolation methods and therefore break down when the response data contains noise [19, 20, 32, 33]. There are approximation and regression methods, e.g. MLS

and MARS, which can be used when the response data contains noise. The formulation of Kriging can even be modified to change it to a regression method [19, 20, 32, 33].

The disadvantage of these methods is that they do not allow for a direct way to separate the noise from the data. Thus, when using them to predict response values, it is not known how much noise there may be in the predicted response value. If these regression surrogate models are used for MCS prediction for reliability analysis, this will affect the amount of uncertainty and variability that there is in the reliability analysis. It is not clear or easy to distinguish if the variability in the reliability analysis is due to the noise in the predicted response or due to the uncertainty in the surrogate model itself. Another disadvantage of these methods is that they do not have a systematic way of characterizing the uncertainty of the surrogate model, the noise in the response value, or the uncertainty in the predicted response values using the surrogate model. Therefore, a surrogate modeling method that can systematically characterize all of these uncertainties as well as accurately predict the true underlying response value without noise needs to be investigated. Bayesian statistical methods allow a natural and systematic way of characterizing uncertainty when estimating both unknown parameters of distributions and other quantities of interest that depend on these unknown distribution parameters.

In this paper a new modified Bayesian Kriging (MBKG) surrogate modeling method is developed for handling performance measures of noisy simulations, which will accurately represent the true underlying unknown performance function without noise. The likelihood for the MBKG is proposed, and the prior distributions to be used with the likelihood to fit the Bayesian model are presented. When possible, conjugate prior distributions are used to help simplify the full conditional distributions and to ease the computational burden of fitting the surrogate model. Using the full conditional distributions with a Gibbs sampling algorithm [34], Markov chain Monte Carlo is used to fit the MBKG surrogate model. Computer simulations of engineering models are often computationally expensive; therefore, it is necessary to reduce the number of design of experiment (DoE) samples needed. An efficient DoE sampling method using the credible sets of the MBKG model is developed to systematically reduce the uncertainty in the surrogate model. Finally the developed MBKG surrogate modeling method together with the developed sequential sampling method are demonstrated using a 2-D mathematical example and a 3-D multibody dynamics engineering block-car example. It is shown how the posterior distribution of the probability of failure is improved efficiently.

## 2. REVIEW OF BAYESIAN STATISTICS

### 2.1 Likelihood and Prior Distributions

In real-world problems there is often data available or obtainable that is known or assumed to come from a given distribution type, e.g., the data is known to follow a normal distribution. The distribution from which the data comes is referred to as the sampling distribution or data distribution [35, 36]. However, even when the distribution type of the data is

known, the parameter values of the distribution are often unknown. When the data distribution is considered as a function of the unknown distribution parameters for a given data set, it is referred to as the likelihood function [35-38].

The goal in Bayesian statistics is to come up with an estimate of the unknown parameter values using both the available data and prior knowledge about the unknown parameters. In Bayesian statistics the unknown parameters are treated as if they are random variables. Any prior knowledge or belief about the unknown parameter is expressed using a probability distribution. The definition of subjective probability of an event given by [37] is: “A probability of an event or of the truth of a statement is a number between 0 and 1 that quantifies a particular person’s subjective opinion as to how likely that event is to occur (or to have already occurred) or how likely the statement is to be true.” Similarly, a subjective probability distribution quantifies one’s knowledge about an unknown parameter that may take on any value in a continuum. These probability distributions that express one’s knowledge about the unknown parameters are referred to as the prior distributions or simply as the priors [35-38]. A Bayesian analysis is carried out to update one’s subjective probability distribution of the unknown parameters by combining prior information with the new information contained in the data. The next section will describe how Bayes’ rule is used with the likelihood and prior distributions to calculate the posterior distribution.

## 2.2 Bayes’ Rule and Posterior Distributions

Bayes’ rule provides a way to mathematically and systematically update one’s subjective probability distribution on model parameters. All knowledge available before the current data is observed is encapsulated in the prior. The updating occurs by incorporating the new data contained in the likelihood. Bayes’ rule states that the posterior probability distribution of model parameters given the data is proportional to the product of the likelihood and prior probability distribution [35-38]. Mathematically this can be written as shown in Eq. (1).

$$f(\text{Parameter} | \text{Data}) \propto f(\text{Parameter}) \times f(\text{Data} | \text{Parameter}) \quad (1)$$

The final probability distribution given on the left side of Eq. (1) is called the posterior distribution, often referred to as the posterior. The posterior distribution expresses the current state of knowledge about model parameters. The posterior distribution can be used to obtain desired values about the parameter, e.g., the mean or median of the posterior could be used as a point estimate for the unknown parameter value. The posterior variance reveals the amount of uncertainty that remains about the parameter value—the larger the variance, the larger the uncertainty about what the true parameter value is. The posterior can also be used to give probability intervals, called credible sets, which are believed to contain the true parameter value with the specified probability, e.g., the 95% credible set for the parameter can easily be obtained from the posterior. Credible sets have a

slightly different meaning than confidence intervals. For the 95% credible set, the probability that the true value of the parameter is in that interval is 95%. A 95% confidence interval means that, if the same experiment or test is repeated many times to generate many different data sets and each data set is used to generate a 95% confidence interval, only 95% of the confidence intervals generated would capture the true parameter value, while 5% of the confidence intervals generated would not capture the true parameter value [35, 37]. The next section will discuss the use of conjugate priors and Markov chain Monte Carlo for updating the posterior distribution.

## 2.3 Conjugate Priors and Markov Chain Monte Carlo

The product of the prior distribution and likelihood is used in Bayes’ rule to construct the posterior distribution of the unknown parameter(s). When possible, it is desirable to choose the prior distribution from a parametric family that takes on the same functional form as the likelihood function for the unknown parameter(s); priors of such a form are called conjugate priors. The parameters of the prior distribution are then chosen such that the prior reflects the known information and beliefs about the unknown parameter(s). When applying Bayes’ rule to the likelihood with a conjugate prior, the posterior distribution will belong to the same parametric family as the prior, i.e., the posterior distribution type will be the same distribution type as the prior. The parameter values of the posterior distribution will be a combination of the prior parameter values and the data used for the Bayesian analysis [35-37].

There are scenarios in which a conjugate prior does not exist for a given problem, e.g., a conjugate prior does not adequately reflect the prior knowledge and belief about the unknown parameter(s), or there are multiple unknown parameters for which a conjugate joint distribution does not exist. For such scenarios, any distribution type that reflects the prior knowledge and belief about the unknown parameter(s) can be used as the prior. The use of such priors, however, leads to posterior distributions that most likely are not from a known distributional family. Bayes’ rule can still be applied in such cases but this has to be done using a numerical method.

Markov chain Monte Carlo (MCMC) is a numerical method that can be used to draw samples from high-dimensional and nonstandard probability distributions. One disadvantage of MCMC is that the samples drawn from the distribution are not independent, and this needs to be taken into consideration when using the samples for inference [35-37, 39]. The Markov property states that a sample drawn at a given time point conditional on the sample drawn at the time point immediately before it is independent of all the earlier samples drawn. Under certain regularity conditions, it can be shown that a Markov chain will converge in distribution to samples drawn from the target, i.e., posterior distribution [35, 37, 39]. There is a debate over whether it is better to run one long Markov chain or to run multiple shorter parallel Markov chains starting at different initial values to attempt to determine whether the Markov chain has converged to the target distribution [40]. One common and well-accepted way of diagnosing convergence in distribution

when using MCMC is to use the Brooks, Gelman, and Rubin (BGR) diagnostic [41, 42]. The BGR diagnostic requires running at least two parallel Markov chains starting at over-dispersed initial values. The BGR diagnostic uses the samples drawn from the parallel Markov chains to calculate credible sets of the individual chains using an increasing number of samples from the chain. The parallel chains are also pooled together to form one sample set that is used to calculate credible sets using an increasing number of samples. If widths of the credible sets calculated using the two different methods stabilize and become approximately equal, the MCMC chains are likely to have converged in distribution [37, 41, 42]. It is possible for the BGR diagnostic to misdiagnose convergence, i.e., the BGR diagnostic shows that convergence has been achieved when in actuality convergence has not yet been reached.

### 3. REVIEW OF KRIGING AND DYNAMIC KRIGING

#### 3.1 Kriging Method

The Kriging method is based on the assumption that the response values of interest are a realization from a stochastic process. Consider  $N$  design of experiment (DoE) samples, denoted as  $\mathbf{x}_{DoE} = (\mathbf{x}_1, \mathbf{x}_2, \dots, \mathbf{x}_N)^T$ , and the corresponding  $N$  responses, denoted as  $\mathbf{y} = (y_1, y_2, \dots, y_N)^T$ , where  $\mathbf{x}_{DoE} \in \mathbb{R}^m$  and  $m$  is the number of input variables, i.e., the spatial dimension of the input variables. The Kriging model for the responses is composed of two parts and is expressed mathematically as

$$\mathbf{y} = \mathbf{F}\boldsymbol{\beta} + \mathbf{Z} \quad (1)$$

where  $\mathbf{F}\boldsymbol{\beta}$  is the mean structure of the response,  $\mathbf{F} = [\mathbf{f}_j(\mathbf{x}_i)]$ ,  $i = 1, 2, \dots, N$ ,  $j = 1, 2, \dots, K$  is a  $N \times K$  design matrix where  $\mathbf{f}_j(\mathbf{x}_i)$  is the  $j^{\text{th}}$  basis function evaluated at the  $i^{\text{th}}$  DoE sample point, and  $\boldsymbol{\beta} = [\beta_1, \beta_2, \dots, \beta_K]^T$  are the regression coefficients from the generalized least squares regression method. The second part,  $\mathbf{Z}$ , is a realization from a stationary Gaussian random process with zero mean and covariance function given by

$$\Sigma(\mathbf{x}_i, \mathbf{x}_j) = \sigma^2 R(\boldsymbol{\theta}, \mathbf{x}_i, \mathbf{x}_j) \quad (2)$$

where  $\sigma^2$  is the process variance,  $R$  is the spatial correlation function,  $\boldsymbol{\theta}$  is a vector containing the correlation function parameters, and  $\mathbf{x}_i, \mathbf{x}_j$  are two DoE samples. There are a number of different correlation functions that can be used, e.g., Gaussian, exponential, general exponential, linear, spherical, cubic, and spline. However, for engineering problems, often the Gaussian correlation function is used since it is infinitely differentiable and provides a smooth response surface. The parameters of the Kriging model that best fit the DoE samples and corresponding response values are determined by using the maximum likelihood estimation (MLE) method.

#### 3.2 Dynamic Kriging Method

As previously mentioned, there are a number of different correlation functions to choose from, and there are also numerous basis functions to choose from. It has been shown that for different problems and data some correlation functions fit better than others; it has also been shown that a larger basis function set is not necessarily better than a smaller basis function set [15, 16]. The latest proposed dynamic Kriging method chooses the mean structure from a choice of three mean structures and the correlation function from seven choices that best fit the data [43]. This dynamic Kriging method provides more flexibility and an automated way to build a Kriging model that can fit data from a wide range of problems. However, it is an interpolation method and breaks down when the response values contain noise. Because the standard Kriging and dynamic Kriging methods are interpolation methods they do not accurately predict the true underlying response value when the response values from the simulations contain noise. As more response values are used to build the Kriging models, the standard Kriging method tends to break down, and the surface predicted by the Kriging models becomes very rough.

### 4. MODIFIED BAYESIAN KRIGING (MBKG)

#### 4.1 Modified Bayesian Kriging Formulation

The basic assumption of Kriging is that the response values are realizations from a Gaussian random process. Kriging is commonly referred to as a Bayesian method, though it is typically fitted using MLE methods rather than Bayesian methods. The likelihood for the Bayesian model is the Gaussian random process.

The modified Bayesian Kriging method assumes the response values come from a stationary Gaussian random process with a constant mean structure in the following form:

$$\mathbf{y} \sim MVN(\mu_c \mathbf{1} + \boldsymbol{\phi}, \sigma^2 \lambda \mathbf{I}) \quad (3)$$

where  $\mathbf{y}$  is the vector of response values at the DoE samples. The above formulation states that the response values are conditionally independent given parameters defining a variance of  $\sigma^2 \lambda$  and a mean value of  $\mu_c \mathbf{1} + \boldsymbol{\phi}$ , which is composed of two parts, the first part is a constant value of  $\mu_c$ , and the second part is  $\boldsymbol{\phi}$ , which depends on the spatial correlation of the DoE samples  $\mathbf{x}$ ; this is expressed mathematically as

$$\boldsymbol{\phi} \sim MVN(\mathbf{0}, \sigma^2 \boldsymbol{\Psi}) \quad (4)$$

where  $\sigma^2 \boldsymbol{\Psi}$  is the covariance of the Gaussian process,  $\sigma^2$  is the variance of the  $\boldsymbol{\phi}$  values, and  $\boldsymbol{\Psi}$  is the spatial correlation matrix. Similar to the Kriging method, the spatial correlation matrix is a function of the DoE samples  $\mathbf{x}$  via the correlation function that is used. The Gaussian correlation function is the most commonly used for engineering problems and is defined as

$$\Psi^{(i)} = \exp\left(-\sum_{j=1}^k \theta_j |x_j^{(i)} - x_j|^2\right) \quad (5)$$

where  $\theta_j$  is the  $j^{\text{th}}$  correlation function parameter corresponding to the  $j^{\text{th}}$  dimension,  $k$  is the number of spatial dimensions,  $x_j$  is the value of DoE sample for the  $j^{\text{th}}$  dimension, and superscript  $i$  is for the  $i^{\text{th}}$  DoE sample. Table 1 lists seven different correlation functions from the literature [43].

Table 1. Correlation Functions

Name	$\Psi^{(i)}$
Gaussian	$\exp\left(-\sum_{j=1}^k \theta_j  x_j^{(i)} - x_j ^{p_j}\right)$
Exponential	$\exp\left(-\theta_j  x_j^{(i)} - x_j \right)$
General Exponential	$\exp\left(-\theta_j  x_j^{(i)} - x_j ^{\theta_{n+1}}\right), 0 < \theta_{n+1} \leq 2$
Linear	$\max\{0, 1 - \theta_j  x_j^{(i)} - x_j \}$
Spherical	$1 - 1.5\xi_j + 0.5\xi_j^3, \xi_j = \min\{1, \theta_j  x_j^{(i)} - x_j \}$
Cubic	$1 - 3\xi_j^2 + 2\xi_j^3, \xi_j = \min\{1, \theta_j  x_j^{(i)} - x_j \}$
Spline	$\begin{cases} 1 - 15\xi_j^2 + 30\xi_j^3, & \text{for } 0 \leq \xi_j \leq 0.2 \\ 1.25(1 - \xi_j)^3, & \text{for } 0 < \xi_j < 1 \\ 0, & \text{for } \xi_j \geq 1, \end{cases}$ where $\xi_j = \theta_j  x_j^{(i)} - x_j $

The unknown MBKG parameters that need to be determined in order to fit the model to the data, i.e., fit the model to the DoE samples  $\mathbf{x}$  and their corresponding response values  $\mathbf{y}$ , are  $\mu_c$ ,  $\sigma^2$ ,  $\lambda$ , and  $\boldsymbol{\theta}$ . The dimension of the  $\boldsymbol{\theta}$  vector is the same as the spatial dimension of  $\mathbf{x}$ . From the Bayesian perspective, the likelihood of the response values is the Gaussian process given in Eq. (3), and the prior for the  $\boldsymbol{\phi}$  vector is the Gaussian process given in Eq. (4). The prior distributions for the remaining unknown parameters will be presented in the next section.

The modified Bayesian Kriging method can also be formulated to have a mean structure that is a function of the DoE samples  $\mathbf{x}$ . For this formulation Eq. (3) is modified to give:

$$\mathbf{y} \sim MVN(\boldsymbol{\mu} + \boldsymbol{\phi}, \sigma^2 \boldsymbol{\lambda} \mathbf{I}) \quad (6)$$

where  $\mu_c \mathbf{1}$  is replaced by the vector  $\boldsymbol{\mu}$ , which is a function of the DoE sample points. The  $\boldsymbol{\mu}$  vector is expressed as:

$$\boldsymbol{\mu} = \mathbf{F}\boldsymbol{\beta} \quad (7)$$

where  $\mathbf{F}$  is the design matrix composed of the polynomial basis functions evaluated at the DoE sample points. For first order the design matrix  $\mathbf{F}$  is expressed as

$$\mathbf{F} = \begin{bmatrix} 1 & x_1^{(1)} & \cdots & x_n^{(1)} \\ 1 & x_1^{(2)} & & x_n^{(2)} \\ \vdots & & \ddots & \vdots \\ 1 & x_1^{(m)} & \cdots & x_n^{(m)} \end{bmatrix}_{m \times (n+1)} \quad (8)$$

where  $m$  is the number of DoE and  $n$  is the number of variables, i.e., the dimension of the problem, and  $\boldsymbol{\beta}$  is a vector of unknown coefficients to be determined when fitting the MBKG surrogate model.

#### 4.2 Prior Distributions for MBKG Parameters

For the three unknown parameters  $\mu_c$ ,  $\sigma^2$ , and  $\lambda$ , semi-conjugate prior distributions are used to help improve the efficiency of fitting the MBKG surrogate model. For the  $\mu_c$  parameter, the conjugate prior distribution is a normal distribution and is expressed as

$$\mu_c \sim N(\mu_p, \sigma_p^2) \quad (9)$$

where  $\mu_p$  and  $\sigma_p^2$  are the prior mean and variance of the  $\mu_c$  parameter, respectively. The conjugate prior distribution for the  $\sigma^2$  parameter is an Inverse-Gamma distribution and is expressed as

$$\sigma^2 \sim \text{InverseGamma}(\alpha_\sigma, \beta_\sigma) \quad (10)$$

where  $\alpha_\sigma$  and  $\beta_\sigma$  are the prior parameters for the distribution. The conjugate prior for the  $\lambda$  parameter is also an Inverse-Gamma distribution and is expressed as

$$\lambda \sim \text{InverseGamma}(\alpha_\lambda, \beta_\lambda) \quad (11)$$

where  $\alpha_\lambda$  and  $\beta_\lambda$  are the prior parameters for the distribution. The  $\boldsymbol{\theta}$  parameters are embedded in the correlation matrix, and because of this there is no known conjugate distribution type that can be used for the prior distribution. Thus, the prior distribution for each of the  $\boldsymbol{\theta}$  parameters is chosen to be a uniform distribution and is expressed as

$$\theta_j \sim U(a_{\theta_j}, b_{\theta_j}) \quad (12)$$

where  $\theta_j$  is the  $j^{\text{th}}$  correlation function parameter, and  $a_{\theta_j}$  and  $b_{\theta_j}$  are the prior parameters for  $\theta_j$ .

If the mean structure is not constant, then the  $\boldsymbol{\mu}$  vector is used as in Eq. (7) and the conjugate prior is a multivariate normal distribution and is expressed as

$$\boldsymbol{\beta} \sim MVN(\boldsymbol{\mu}_\beta, \boldsymbol{\Sigma}_\beta) \quad (13)$$

where  $\boldsymbol{\mu}_\beta$  and  $\boldsymbol{\Sigma}_\beta$  are the prior mean vector and covariance matrix for the distribution.

Prior to fitting the MBKG model, the response values  $\mathbf{y}$  are normalized such that they have a zero mean. The normalization is expressed as

$$y_i = \frac{\tilde{y}_i - \text{mean}(\tilde{\mathbf{y}})}{\text{std}(\tilde{\mathbf{y}})} \quad (14)$$

where  $y_i$  is the normalized response value of the  $i^{\text{th}}$  response,  $\tilde{y}_i$  is the original response value for the  $i^{\text{th}}$  response,  $\text{mean}(\tilde{\mathbf{y}})$  is the mean of the original response values, and  $\text{std}(\tilde{\mathbf{y}})$  is the standard deviation of the original response value. The DoE samples are also normalized in the same way as the response values. In the literature it has been found that, when fitting surrogate models, a better fit can usually be achieved when the DoE samples and response values are normalized in some way to help restrict the range of the possible values than when they are not normalized [20].

In addition to the normal distribution being a conjugate prior for the  $\mu_c$  parameter, it is also a good choice because of the normalization of the response values. It is expected that the overall mean of the normalized response values should be close to zero. Thus, a normal distribution with a zero mean and a standard deviation of 0.5 is a prior distribution that reflects this knowledge. This prior distribution can still be considered a relatively noninformative prior distribution; thus, it can be used in general when creating a surrogate model for any problem.

The Inverse-Gamma distribution has positive support, meaning that the random variable of an Inverse-Gamma distribution can only take on positive values. From Eqs. (3) and (4) it can be seen that both parameters  $\sigma^2$  and  $\lambda$  are variance parameters to a Gaussian process; therefore, by definition they can only take on positive values. With the Inverse-Gamma distribution being a positive value distribution and a conjugate prior for both  $\sigma^2$  and  $\lambda$ , it is ideally suited to be used as the prior distribution.

A uniform distribution for the  $\boldsymbol{\theta}$  parameters was chosen mostly because it gives a direct way to limit the possible values

that the  $\boldsymbol{\theta}$  parameters can take on. Due to the normalization of the DoE samples, the maximum distance in each of the spatial directions from any given DoE sample to all the others is roughly three. After studying the Gaussian correlation function closely, it was found that a  $\theta$  value of five and greater produces a correlation value that is asymptotically approaching zero regardless of the distance between the DoE samples. This is shown in Fig. 1, where the vertical axis is the squared distance between DoE sample points, and the horizontal axis is the correlation function parameter  $\theta$ . As seen in the Fig.1, when  $\theta \approx 2.5$  and the squared distance is greater than one, the correlation is smaller than 0.1. Also seen in the Fig. 1 is that when  $\theta=5$ , the correlation is smaller than 0.1 except for squared distances that are approximately less than 0.5. Given this study, it was determined that an appropriate upper bound would be  $\theta=5$  and an appropriate lower bound would be  $\theta=0.15$ , these are the bounds used in the uniform prior distribution.

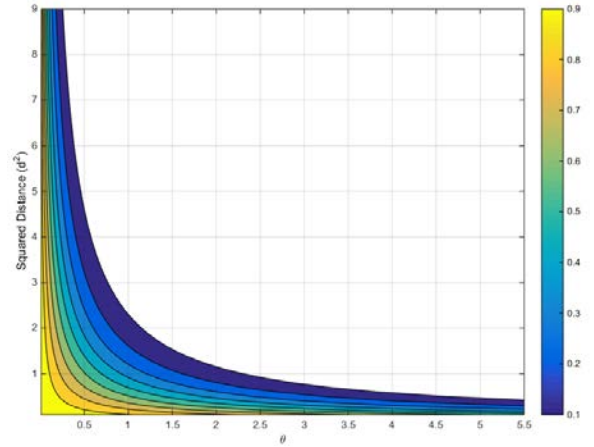


Figure 1. Correlation Contour of the Gaussian Correlation Function

#### 4.3 Full Conditional Distributions for MBKG Parameters

The joint posterior distribution of the unknown parameters in a Bayesian model is needed to derive the full conditional distributions of the unknown parameters being estimated. The joint posterior distribution for the MBKG formulation given in Eq. (6) is expressed as

$$f(\mu_c, \sigma^2, \boldsymbol{\theta}, \lambda, \boldsymbol{\phi} | \mathbf{y}) \propto \prod_{j=1}^k [U(a_{\theta_j}, b_{\theta_j})]^* \text{InverseGamma}(\alpha_\sigma, \beta_\sigma)^* N(\mu_p, \sigma_p^2)^* \text{InverseGamma}(\alpha_\lambda, \beta_\lambda)^* MVN(\boldsymbol{\theta}, \sigma^2 \boldsymbol{\Psi})^* MVN(\boldsymbol{\mu} + \boldsymbol{\phi}, \sigma^2 \lambda \mathbf{I}) \quad (15)$$

The derivation of the full conditional distributions these distributions is not new work and therefore in the interest of

space are not repeated in this paper. However, the full conditionals for each of the parameters are given. The full conditional for  $\sigma^2$  can be shown to be

$$f(\sigma^2 | \mathbf{y}, \mu_c, \boldsymbol{\theta}, \lambda, \boldsymbol{\varphi}) \sim \text{InverseGamma}\left(\alpha_\sigma + n, \beta_\sigma + \frac{1}{2} \boldsymbol{\varphi}^T \boldsymbol{\Psi}^{-1} \boldsymbol{\varphi} + \frac{1}{2} \frac{1}{\lambda} (\mathbf{y} - \boldsymbol{\mu} - \boldsymbol{\varphi})^T (\mathbf{y} - \boldsymbol{\mu} - \boldsymbol{\varphi})\right) \quad (16)$$

The full conditional for  $\lambda$  can be shown to be

$$f(\lambda | \mathbf{y}, \mu_c, \sigma^2, \boldsymbol{\theta}, \boldsymbol{\varphi}) \sim \text{InverseGamma}\left(\alpha_\lambda + \frac{n}{2}, \beta_\lambda + \frac{1}{2} \frac{1}{\sigma^2} (\mathbf{y} - \boldsymbol{\mu} - \boldsymbol{\varphi})^T (\mathbf{y} - \boldsymbol{\mu} - \boldsymbol{\varphi})\right) \quad (17)$$

The full conditional for the  $\theta_j$  parameter can be shown to be

$$\text{Ln}\left[f(\theta_j | \mathbf{y}, \mu_c, \sigma^2, \boldsymbol{\theta}_{j-}, \lambda, \boldsymbol{\varphi})\right] \propto -\frac{n}{2} \text{Ln}[\sigma^2] - \frac{1}{2} \text{Ln}[\boldsymbol{\Psi}] + \left(-\frac{1}{2} \boldsymbol{\varphi}^T \boldsymbol{\Sigma}^{-1} \boldsymbol{\varphi}\right) \quad (18)$$

To draw samples from the nonstandard distribution given in Eq. (17), the Metropolis-Hastings algorithm [44, 45] will be used. For numerical stability, the natural logarithm of the full conditional is used with the Metropolis-Hastings algorithm.

The full conditional distribution for  $\boldsymbol{\varphi}$  can be shown to be

$$f(\boldsymbol{\beta} | \mathbf{y}, \sigma^2, \lambda, \boldsymbol{\theta}, \boldsymbol{\varphi}) \sim \text{MVN}(\boldsymbol{\gamma}, \mathbf{A}^{-1}) \quad (19)$$

where  $\boldsymbol{\gamma}$ ,  $\mathbf{A}$ , and  $\mathbf{b}$  are defined in Eqs. (20), (21), and (22) respectively.

$$\boldsymbol{\gamma} = \frac{1}{2} \mathbf{A}^{-1} \mathbf{b} \quad (20)$$

$$\mathbf{A} = \left( \frac{1}{\sigma^2 \lambda} \mathbf{F}^T \mathbf{F} + (\boldsymbol{\Sigma}_\beta)^{-1} \right) \quad (21)$$

$$\mathbf{b} = 2 \left( (\boldsymbol{\mu}_\beta)^T (\boldsymbol{\Sigma}_\beta)^{-1} - \frac{1}{\sigma^2 \lambda} (\boldsymbol{\varphi}^T - \mathbf{y}^T) \mathbf{F} \right) \quad (22)$$

The full conditional distribution for  $\boldsymbol{\beta}$  can be shown to be

$$f(\boldsymbol{\beta} | \mathbf{y}, \sigma^2, \lambda, \boldsymbol{\theta}, \boldsymbol{\varphi}) \sim \text{MVN}(\boldsymbol{\gamma}, \mathbf{A}^{-1}) \quad (22)$$

## 5. SEQUENTIAL SAMPLING VIA CREDIBLE SETS

Recall that the objective of developing the MBKG surrogate modeling method is so that it can be used for carrying out reliability analyses. When using surrogate models to carry out reliability analysis it is common practice to normalize the response values such that failure is defined to be when the response value is greater than zero. This zero boundary that separates the failure and safe region is called the limit state. Thus, in order to use an MBKG surrogate model for carrying out a reliability analysis, the accuracy of the limit state function is of high importance because it will dictate the accuracy of the reliability analysis. A sequential sampling method is developed for adding more design of experiment (DoE) samples to further improve the modified Bayesian Kriging (MBKG) surrogate model by utilizing the information in the posterior credible sets of the MBKG surrogate model. The method is developed such that it improves the accuracy of the limit state as more DoE samples are added.

The MBKG surrogate model is not a deterministic surrogate model, but rather a surrogate model that produces posterior distributions for the MBKG parameters. Therefore, a predicted response value for a given point does not have one deterministic value but rather has a probability distribution that gives the probability of the predicted response value being in any interval. The Markov chain Monte Carlo (MCMC) samples drawn from the predictive distribution of the response variable can be used to estimate any desired characteristic of the distribution, e.g., the mean, standard deviation, and credible sets. The larger the standard deviation and the wider the credible set, the more uncertainty there is in the predicted value, i.e., more uncertainty in what the true value is. The probability distributions characterize this uncertainty and provide information that can be used to further improve the MBKG surrogate model.

When adding new DoE samples to improve the MBKG surrogate model, it is desirable to place them far from the existing samples so that they will contribute more information to the model. It is also desirable to place them at locations where the amount of uncertainty in the limit state is the largest. Placing the new DoE samples in this strategic way will provide the maximum amount of information to the MBKG surrogate model and, thus will require fewer DoE samples to be used to fit the MBKG surrogate model.

To select the DoE samples to fit the MBKG surrogate model, random uniform samples are generated throughout the domain of the variables and are referred to as test points. That is, 500 random uniform test points may be generated for a 2-D or 3-D problem. After the test points are created, a small number, e.g., 25, of the test points are selected randomly so that they uniformly cover the domain of the variables. These initially selected test points are then used to fit the MBKG surrogate model. After the MBKG surrogate model has been fitted, all of the test points are then used to generate the predictive distribution for each response value corresponding to each test point. These predictive distributions characterize the uncertainty in the predicted response values. The wider the distribution, the more uncertainty in the response value.

To reduce the uncertainty in the limit state, it is desirable to select test points whose predicted responses have 95% credible sets that contain zero and are wide. If the credible set contain zeros this indicates that the limit state may be near by the test point. If the credible set is wide this indicates there is a large amount of uncertainty in the predicted response. Test points with these two characteristics are ideal candidates for being new additional DoE samples that can be used to fit the MBKG surrogate model as they will add the most information to the surrogate model. These additional DoE samples can then be used together with the initial DoE samples to refit the MBKG surrogate model. This process can be done iteratively to sequentially select DoE samples to be used to fit the MBKG surrogate model.

It is also desirable to select the sequentially added DoE samples such that they are far from existing DoE samples so that they will contribute the most information to the MBKG surrogate model. When using a Kriging method it is desirable for DoE samples to be far from existing samples to avoid computational problems with evaluating the correlation matrix. As the distance between DoE samples approaches zero, the estimated correlation approaches one. This causes the correlation matrix to become ill-conditioned and leads to the correlation matrix becoming singular. In this paper it is assumed that the true underlying surface without noise is smooth. Thus, DoE samples that are extremely close to each are likely to have response values that are close to each other. These DoE samples and response values will provide little information to improve the surrogate model. Therefore, it is desirable for sequentially added DoE samples to be far from existing DoE samples to avoid numerical difficulties and also to add the most information to farther improve the surrogate model.

To determine the locations for the sequentially added DoE samples, a weighting system is used. The first step is to calculate the distance between the test points and the existing DoE samples previously used to fit the MBKG surrogate model. This gives a matrix of distance values and can be expressed mathematically as

$$D_{ij} = \|\mathbf{s}^j - \mathbf{t}^i\| \quad \text{for } i = 1, \dots, n_{test} \text{ and } j = 1, \dots, n_{DoE} \quad (23)$$

where  $D_{ij}$  is the distance between the  $i^{th}$  test point and  $j^{th}$  existing DoE sample,  $\mathbf{s}^j$  is the  $j^{th}$  existing DoE sample,  $\mathbf{t}^i$  is the  $i^{th}$  test point,  $n_{test}$  is the number of test points whose 95% credible set capture zero, and  $n_{DoE}$  is the number of existing DoE samples. Once these distances are obtained, the next step is to find the minimum distance from all the existing DoE samples for each test point. This then gives a vector of the distance between the test point and the closest existing DoE sample, which is expressed mathematically as

$$d_i = \min \{D_{ij}\} \quad \text{for } j = 1, \dots, n_{DoE} \quad (24)$$

where  $d_i$  is the distance between the  $i^{th}$  test point and the closest existing DoE sample,  $D_{ij}$  is the distance between the  $i^{th}$  test point and the  $j^{th}$  existing DoE sample as calculated in Eq. (23), and  $n_{DoE}$  is the number of existing DoE samples.

The last value needed to calculate the weight is the width of the 95% credible sets that capture zero. This width is simply calculated as

$$c_i^w = |c_i^L| + c_i^U \quad \text{for } i = 1, \dots, n_{test} \quad (25)$$

where  $c_i^w$  is the width of the 95% credible set for the  $i^{th}$  test point,  $c_i^L$  is the lower bound of the 95% credible set for the  $i^{th}$  test point,  $c_i^U$  is the upper bound of the 95% credible set for the  $i^{th}$  test point, and  $n_{test}$  is the number of test points. Note that only the 95% credible sets that contain zero are used. Therefore the lower bound,  $c_i^L$ , is always less than zero and upper bound,  $c_i^U$ , is always greater than zero. The weight for each test point is then calculated as

$$w_i = d_i * c_i^w \quad \text{for } i = 1, \dots, n_{test} \quad (26)$$

where  $w_i$  is the weight for the  $i^{th}$  test point,  $d_i$  is the distance between the  $i^{th}$  test point and the closest existing DoE sample as calculated in Eq. (24),  $c_i^w$  is the width of the 95% credible set for the  $i^{th}$  test point as calculated in Eq. (25), and  $n_{test}$  is the number of test points. The test point that has the largest weight given by Eq. (26) is selected as the new DoE sample, expressed as

$$\mathbf{s}^{new} = \max \{w_i\} \quad \text{for } i = 1, \dots, n_{test} \quad (27)$$

where  $\mathbf{s}^{new}$  is the new DoE sample selected from the  $n_{test}$  test points, and  $w_i$  is the weight for the  $i^{th}$  test point. Then  $\mathbf{s}^{new}$  is added to the list of existing DoE samples, and this selection process can be iterated until the desired number of new DoE samples are added.

## 6. EXAMPLES

### 6.1 Nonlinear 2-D Mathematical Example

A 2-D mathematical example with added random noise is used to demonstrate the developed MBKG surrogate modeling and sequential sampling method. The function considered is defined as

$$\begin{aligned} G_2(X) = & -1 + (0.9063X_1 + 0.4226X_2 - 6)^2 \\ & + (0.9063X_1 + 0.4226X_2 - 6)^3 \\ & - 0.6(0.9063X_1 + 0.4226X_2 - 6)^4 \\ & - (-0.4226X_1 + 0.9063X_2) \end{aligned} \quad (28)$$

where  $X_1$  and  $X_2$  are the two input variables. The random noise added to Eq. (28) is generated using a normal distribution with zero mean and a standard deviation of  $\sigma_\varepsilon$  as

$$\varepsilon \sim N(0, \sigma_\varepsilon^2) \quad (29)$$

The response values with noise are then calculated as a summation of the true response value without noise as given by Eq. (28) and a realization of  $\varepsilon$  from the distribution in Eq. (29). This is expressed as

$$y_i = G_2(\mathbf{x}_i) + \varepsilon_i \quad (30)$$

where  $y_i$  is the  $i^{\text{th}}$  response value with noise at  $\mathbf{x}_i$ , which is the  $i^{\text{th}}$  DoE sample point, and  $\varepsilon_i$  is the  $i^{\text{th}}$  realization of noise.

The reliability analysis of Eq. (30) is to be carried out using the two input variables  $X_1$  and  $X_2$ . To carry out the reliability analysis the two input variables are assumed to each follow a normal distribution as

$$\begin{aligned} X_1 &\sim N(5.19, 0.3^2) \\ X_2 &\sim N(0.74, 0.3^2) \end{aligned} \quad (31)$$

and are correlated to each other by Clayton copula with a correlation coefficient of 0.5. Because of this correlation the domain of interest for this example forms the raindrop shape seen in Fig. 2. This domain of interest is referred to as the local window [48].

Thus, when fitting the MBKG surrogate model a local window based on the distributions in Eq. (31) and the Clayton copula correlation was used. It should be noted that the correlation of  $X_1$  and  $X_2$  is used only to construct the local window, i.e., the domain of the MBKG surrogate model. The correlation is not used and does not affect the fitting of the MBKG surrogate model. By using a local window, the DoE samples used to fit the MBKG surrogate model only need to be within the domain of the local window and not the entire domain of  $X_1$  and  $X_2$  for Eq. (28).

To start the fitting process of the MBKG surrogate model, 1000 uniform randomly generated test points were generated in the local window as shown in Fig. 2. The black filled circle in Fig. 2 is the location of the mean value for  $X_1$  and  $X_2$  as given in Eq. (31).

The DoE samples used to fit the MBKG surrogate model are selected from among the test points shown in Fig. 2. The initial 25 DoE samples used to initially fit the MBKG surrogate model were selected such that they uniformly covered the domain and are shown in Fig. 3 as the blue circles. The contour of the true limit state of Eq.

(28) is also shown in Fig. 3 as the red curve. Using the DoE samples and Eq. (30), response values are generated and used to fit the MBKG surrogate model.

For the MBKG surrogate model, a second order mean structure and the spline correlation function were used. The values used for the prior parameters are given in Table 2. Markov chain Monte Carlo (MCMC) was carried out using the 25 initial DoE and response values given by Eq. (30), where  $\sigma_\varepsilon = 0.01$  was used with Eq. (29) to generate the noise in the response. Three parallel chains, each of 150,000 iterations were generated using MCMC. The first 100,000 iterations were discarded as burn-in.

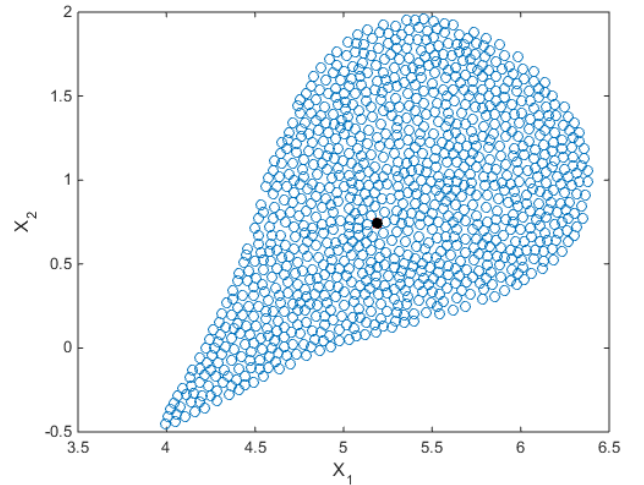


Figure 2. A 1000 Uniform Randomly Generated Test Points

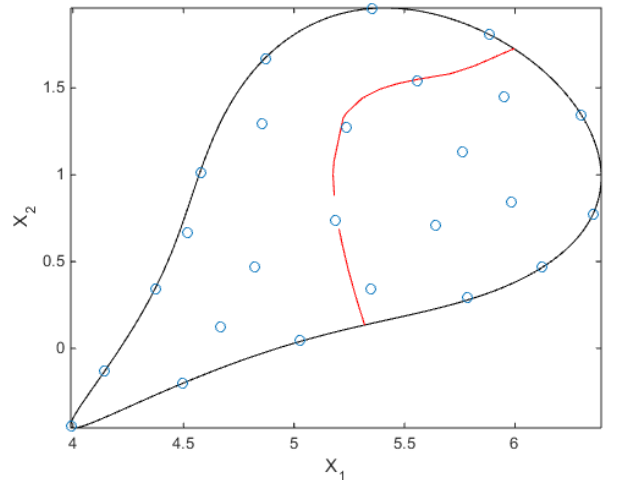


Figure 3. Initial 25 DoE and Limit State of Eq. (28)

Table 2. Prior Parameter Values for Fitting Eq. (30)

Unknown Parameter	Prior Distribution	Parameter 1	Parameter 2
$\beta$	M.V. Normal	$\mu_\beta = \mathbf{0}$	$\Sigma_\beta = 650\mathbf{I}$
$\sigma^2$	Inverse-Gamma	$\alpha_\sigma = 2.0000$	$\beta_\sigma = 2.500$
$\lambda$	Inverse-Gamma	$\alpha_\lambda = 1.9548$	$\beta_\lambda = 0.2747$
$\theta_i$	Uniform	$a_{\theta_i} = 0.1500$	$b_{\theta_i} = 5.0000$

To generate the contour plot of the limit state, response values were predicted using the fitted MBKG surrogate model. The mean values of the response values were then used to generate the contour plot of limit state given by the MBKG surrogate model. The predicted limit state is shown in Fig. 4 as the green curve. It is easily seen that the initial prediction of the limit state does not match the true limit state (red curve in Fig. 4) very well. To improve the prediction of the limit state the sequential sampling method developed in Section 5 will be used to select 20 more DoE samples. The blue circles in Fig. 4 are the initial 25 DoE samples used. The yellow filled circles in Fig. 4 are the test points whose 95% credible set of the predicted response value capture zero. As seen in Fig. 4 the yellow filled circles cover a large portion of the local window. This indicates that there is a large amount of uncertainty in the predicted response values. Using the sequential sampling method developed in Section 5, 20 more DoE samples are selected. The 20 additional DoE samples are shown in Fig. 4 as the black squares. It is seen how the 20 additional DoE samples are selected such that they are roughly uniformly spaced from the existing 25 initial DoE samples. Using the 45 DoE samples the MBKG surrogate model is refitted. The contour of the limit state given by MBKG surrogate model using the 45 DoE samples is shown as the blue curve in Fig. 4. The test points are predicted again using the updated MBKG surrogate model. The test points whose 95% credible set that capture zero are shown as the black dots in Fig. 5. In Fig. 5 it can be seen how the 95% credible set capture the limit state shrank, i.e., the uncertainty about the location of the limit state is smaller.

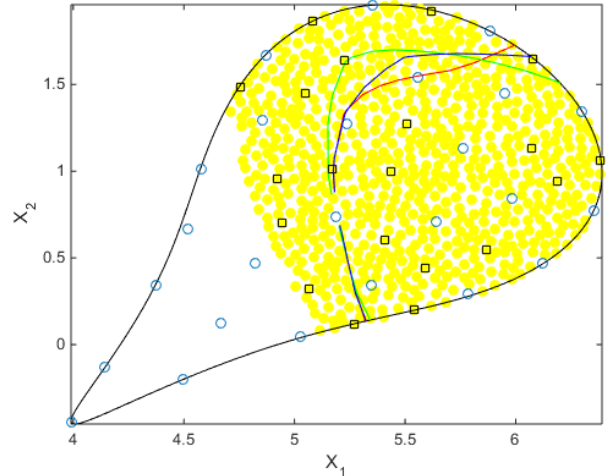


Figure 4. Contours of MBKG Limit State and Test Points with 95% Credible Set Capturing Limit State Using 25 DoE

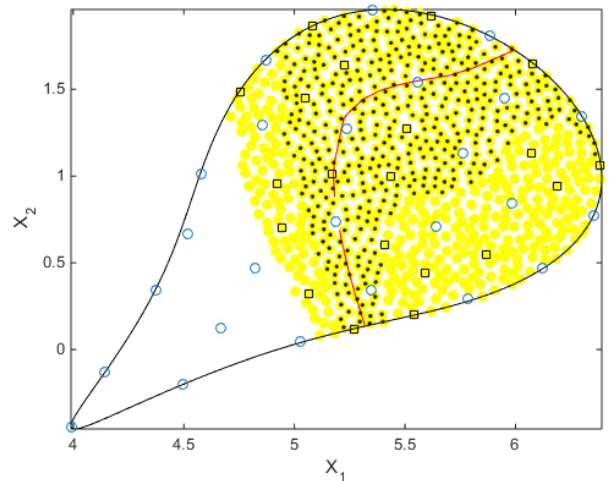


Figure 5. Test Points with 95% Credible Set Capturing Limit State Using 45 DoE

The sequential sampling process is repeated three more times, adding 20 DoE samples each time until a total of 105 DoE samples are used to fit the MBKG surrogate model. Figure 6 shows the true limit state of Eq. (28) as the red curve, the predicted limit state given by the MBKG surrogate model as the blue curve, the initial 25 DoE as the blue circles, the first set of 20 sequential DoE as the black squares, the second set of 20 sequential DoE as the pink circles, the third set of 20 sequential DoE as the blue X's, and the fourth set of 20 sequential DoE as the blue dots.

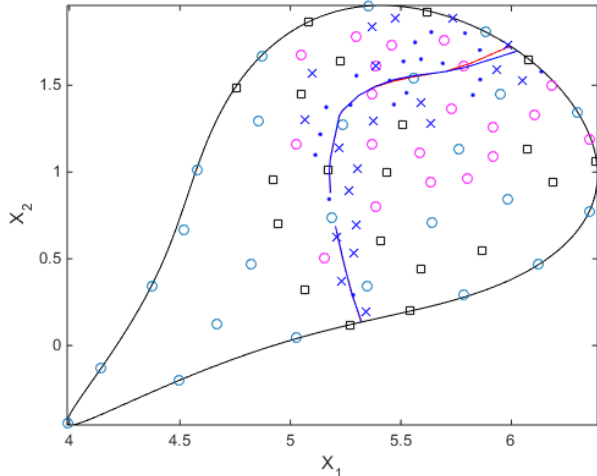


Figure 6. MBKG Limit State and 105 DoE Samples

It was demonstrated visually how the prediction of the limit state is improved using the sequential sampling method. To numerically study how the limit state is improving, a reliability analysis using the MBKG surrogate model is carried out. The probability of failure is predicted for each MCMC iteration. This gives the distribution of the probability of failure. This distribution characterizes the amount of uncertainty in the prediction of the probability of failure. Figure 7 shows the posterior distribution of the probability of failure when only the initial 25 DoE samples are used to fit the MBKG surrogate model. Figure 8 shows the posterior distribution of the probability of failure when 65 DoE samples are used to fit the MBKG surrogate model. The additional 40 DoE samples were added 20 at a time using the sequential sampling method. Figure 9 shows the posterior distribution of the probability of failure when 105 DoE samples are used to fit the MBKG surrogate model. Studying Figs. 7-9 it can be seen that the posterior distribution of the probability of failure is becoming narrower and narrower, indicating that amount of uncertainty is decreasing.

Table 3 shows the probability of failure statistics using the different number of DOE samples. As seen in Table 3 the mean value of the probability of failure is converging to the true probability of failure. Also seen in Table 3 is how the standard deviation of the probability of failure decreases as more DoE samples are used. The 95% credible set of the probability of failure shrinks as more DoE samples are added. The decrease in the standard deviation and the shrinkage of the 95% credible set indicates reflects how there is less uncertainty in the prediction of the probability of failure as more DoE samples are added.

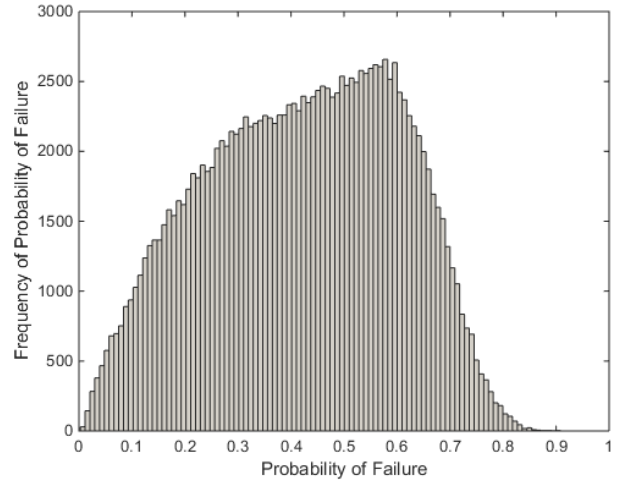


Figure 7. Posterior Distribution of Probability of Failure Using 25 DoE

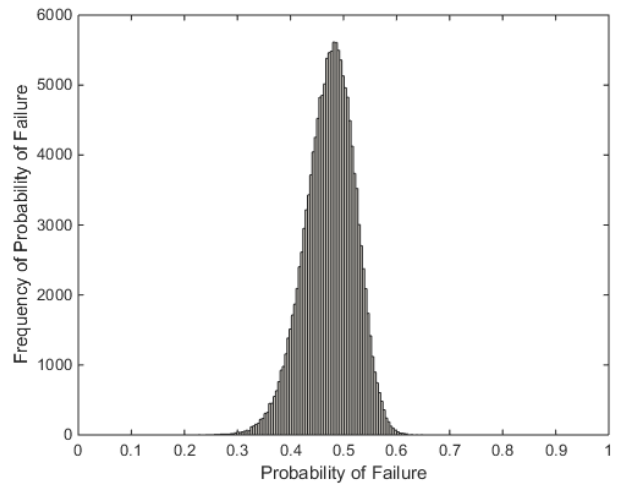


Figure 8. Posterior Distribution of Probability of Failure Using 65 DoE

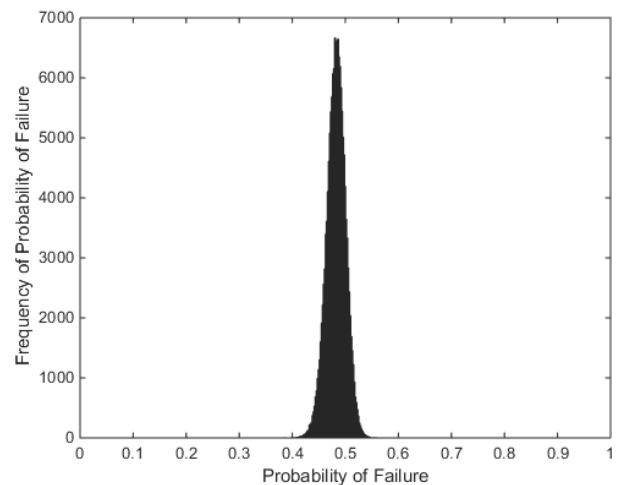


Figure 9. Posterior Distribution of Probability of Failure Using 105 DoE

The above study was done using  $\sigma_\varepsilon = 0.01$  with Eq. (29) to generate the noise in the response. The MBKG surrogate modeling and sequential sampling method was also studied for two higher noise levels of  $\sigma_\varepsilon = 0.05$  and  $\sigma_\varepsilon = 0.1$ . The probability of failure statistics for noise levels when  $\sigma_\varepsilon = 0.05$  and  $\sigma_\varepsilon = 0.1$  are shown in Tables 4 and 5, respectively. From Tables 3-5 it can be seen that the mean value of the probability

of failure is converging to the true probability of failure as the number of DoE increases. It can also be seen that the credible sets for the larger noise are slightly wider than for the smaller noise. This indicates that with the larger noise there is more uncertainty in the prediction of the probability of failure. It can also be seen that the 95% credible sets for all noise levels does in fact capture the true probability of failure. Thus, the method is robust for different levels of noise in the response.

Table 3. Probability of Failure Statistics for  $\sigma_\varepsilon = 0.01$ 

# DoE Samples	Mean	Std.	95% Credible Set	
25	42.12%	0.1809	8.10%	72.75%
45	45.55%	0.0875	25.29%	59.82%
65	47.36%	0.0473	37.32%	55.79%
85	48.15%	0.0253	43.05%	53.00%
105	48.26%	0.0180	44.57%	51.68%
True	48.47%	N/A	N/A	N/A

Table 4. Probability of Failure Statistics for  $\sigma_\varepsilon = 0.05$ 

# DoE Samples	Mean	Std.	95% Credible Set	
25	42.48%	0.1800	8.15%	72.71%
45	46.13%	0.0892	25.17%	60.44%
65	47.52%	0.0471	37.34%	55.75%
85	48.62%	0.0244	43.72%	53.33%
105	48.30%	0.0203	44.10%	52.12%
True	48.47%	N/A	N/A	N/A

Table 5. Probability of Failure Statistics for  $\sigma_\varepsilon = 0.1$ 

# DoE Samples	Mean	Std.	95% Credible Set	
25	42.94%	0.1786	8.42%	72.61%
45	47.64%	0.0865	27.05%	61.34%
65	48.79%	0.0488	38.26%	57.33%
85	47.75%	0.0294	41.51%	53.14%
105	47.98%	0.0233	43.00%	52.19%
True	48.47%	N/A	N/A	N/A

## 6.2 A 3-D Multibody Dynamics Engineering Example

This section will present a 3-D multibody dynamics (MBD) block-car example that uses the developed methods to estimate

the probability of failure for the current design. The problem is a simple example to demonstrate using the method for an actual engineering problem that contains noise in the response. Figure

10 shows the multibody dynamics block-car used for this example. The car is modeled as a simple block with four wheels as shown in Fig. 10. The origin of the local coordinate system for the car body is located at the center of the car body as shown in Fig. 10. Reliability analysis of this example was attempted previously using standard Kriging methods as the surrogate modeling method. However, the standard Kriging methods failed when trying to create the surrogate model for the contact force due to the noise in the contact force response. The standard Kriging method failed in that the predicted response surface was not a smooth surface. The predicted response surface looked like white noise, i.e., it was not smooth and was jagged. This example was the motivation that led to the research carried out in this work and the development of the methods for handling noisy response problems.

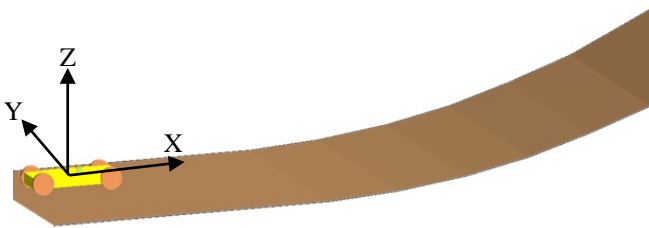


Figure 10. Multibody Dynamics Block-Car Example

The three design variables are the mass of the car and the locations of the center of mass in the  $x$  and  $z$  directions. The two performance measures of interest for this example are the contact forces between the front wheels and the ground. The contact force should not be less than 125 pounds, i.e., failure is defined as the contact force being less than 125 pounds. These constraints are imposed so that the car does not flip over backwards when going up the incline. Contact forces calculated by MBD simulation software are known to be inherently noisy responses. For this example the commercially available MBD software package used was RecurDyn [49]. The values of the three variables for the current design are defined in Table 6. The negative numbers in Table 6 mean that the center of mass is located to the back and the bottom of the car, i.e., the negative  $x$  and  $z$  direction.

Table 6. Current Design of MBD Block-Car

Design Variable	Current Design
$d_1 = Mass$	65.00
$d_2 = CM_x$	-33.92
$d_3 = CM_z$	-43.78

For the MBKG surrogate model a second order mean structure and spline correlation function were used. Three parallel chains, each with 200,000 iterations, were generated

using MCMC. The first 150,000 iterations were discarded as burn-in. The remaining 50,000 iterations were pooled to give a total of 150,000 samples from the posterior distribution to use for inference. The fitting of the MBKG surrogate model started with 25 DoE samples with additional DoE samples added using the developed sequential sampling method.

Tables 7 and 8 show the probability of failure statistics as more DoE samples are added to the MBKG surrogate model. As seen in both tables the standard deviations are large and 95% credible sets are wide when using only 25 DoE samples. This indicates that there is a large amount of uncertainty in the estimation of the probability of failure. The standard deviation decreases as the number of the DoE increases. The 95% credible sets shrink noticeably up until about 105 DoE are added. From 105 DoE samples until 165 DoE samples, the estimates of the mean, standard deviation, and 95% credible set appear to be converging. Thus, the developed methods look to be performing well for this example.

Table 7. Probability of Failure Statistics for Left Front Wheel

# DoE Samples	Mean	Std.	95% Credible Set	
25	38.62%	0.1310	16.35%	66.65%
45	42.94%	0.0756	28.10%	58.16%
65	47.76%	0.0500	38.11%	58.03%
85	44.15%	0.0367	36.72%	51.44%
105	43.19%	0.0320	37.06%	49.62%
125	42.65%	0.0262	37.58%	47.92%
145	43.16%	0.0236	38.67%	47.99%
165	41.22%	0.0223	37.11%	45.82%

Table 8. Probability of Failure Statistics for Right Front Wheel

# DoE Samples	Mean	Std.	95% Credible Set	
25	48.30%	0.1359	23.05%	75.32%
45	55.63%	0.0815	39.43%	71.25%
65	64.38%	0.0492	54.25%	73.64%
85	65.75%	0.0352	58.55%	72.51%
105	63.79%	0.0290	57.91%	69.40%
125	63.23%	0.0225	58.56%	67.54%
145	61.69%	0.0202	57.74%	65.80%
165	59.43%	0.0210	55.28%	63.53%

## 7. CONCLUSION

The use of surrogate models for carrying out reliability analysis is becoming popular. However, interpolation-based surrogate modeling methods break down when the response values contain noise. On the other hand, for regression-based surrogate modeling methods that can handle responses with noise, the uncertainty in the surrogate model and predicted response values is unknown. A modified Bayesian Kriging (MBKG) surrogate modeling method for problems in which simulation analyses are inherently noisy was successfully developed. The MBKG surrogate modeling method was developed to be used to carry out reliability analysis to predict the probability of failure. The posterior distributions generated by the MBKG surrogate model characterize the uncertainty in the estimated parameters. A sequential sampling method that uses the posterior credible sets of the MBKG surrogate model was successfully developed.

As with any method, the developed method does have some limitations. Like all surrogate modeling methods, as the number of dimensions grows, the difficulty and the number of DoE required to build an accurate surrogate model grows. Thus, for a high dimensional problem the MBKG surrogate modeling

method may not be well suited. A more detailed study on how many dimensions the MBKG surrogate modeling method can handle is left as future research to be carried out. The disadvantage of using Markov chain Monte Carlo (MCMC) to fit the MBKG surrogate model is the long computational time required. Each of the MCMC iterations of a chain has to be drawn serially, so if a large number of iterations is required to converge to the posterior distribution, the computational time will be long. However, multiple MCMC chains can be run in parallel to reduce the computational time. Another difficulty with the MBKG surrogate modeling method is determining priors to be used for parameters of the MBKG surrogate model. For the examples presented in this paper relatively noninformative priors were used. However, it might be possible to come up with more informative priors which would reduce the total number of DoE samples required to fit the MBKG surrogate model. Studying the effects of the priors on fitting the MBKG surrogate model is left as future research.

The new methods were demonstrated with a 2-D mathematical example and a 3-D MBD engineering example. The examples showed how the posterior distribution of the probability of failure becomes narrower as more DoE samples

are used. It was also shown that the mean value of the estimated probability of failure converged to the true probability of failure as more DoE samples were sequentially added to the MBKG surrogate model. Thus, the two examples successfully demonstrated the developed methods.

## 8. ACKNOWLEDGEMENTS

The authors wish to acknowledge the technical and financial support of the Automotive Research Center (ARC) in accordance with Cooperative Agreement W56HZV-04-2-0001 U.S. Army Tank Automotive Research, Development and Engineering Center (TARDEC).

## 9. REFERENCES

- [1] Lee, I., Choi, K. K., & Gorsich, D. (2010). System reliability-based design optimization using the MPP-based dimension reduction method. *Structural and Multidisciplinary Optimization*, 41(6), 823-839. doi:10.1007/s00158-009-0459-0
- [2] Lee, I., Choi, K. K., Du, L., & Gorsich, D. (2008). Inverse analysis method using MPP-based dimension reduction for reliability-based design optimization of nonlinear and multi-dimensional systems. *Computer Methods in Applied Mechanics and Engineering*, 198(1), 14-27. doi:http://dx.doi.org/10.1016/j.cma.2008.03.004
- [3] Rahman, S., & Wei, D. (2006). A univariate approximation at most probable point for higher-order reliability analysis. *International Journal of Solids and Structures*, 43(9), 2820-2839. doi:http://dx.doi.org/10.1016/j.ijsolstr.2005.05.053
- [4] Youn, B. D., & Choi, K. K. (2003). An investigation of nonlinearity of reliability-based design optimization approaches. *Journal of Mechanical Design*, 126(3), 403-411. doi:10.1115/1.1701880
- [5] Haldar, A., & Mahadevan, S. (2000). *Probability, reliability, and statistical methods in engineering design*. New York : J. Wiley.
- [6] Tu, J., Choi, K. K., & Park, Y. H. (1999). A new study on reliability-based design optimization. *Journal of Mechanical Design*, 121(4), 557-564. doi:10.1115/1.2829499
- [7] Hohenbichler, M., Gollwitzer, S., Kruse, W., & Rackwitz, R. (1987). New light on first- and second-order reliability methods. *Structural Safety*, 4(4), 267-284. doi:http://dx.doi.org/10.1016/0167-4730(87)90002-6
- [8] Madsen, H. O., Krenk, S., & Lind, N. C. (1985). *Methods of structural safety*. Englewood Cliffs, NJ : Prentice-Hall.
- [9] Hohenbichler, M., & Rackwitz, R. (1988). Improvement of Second-Order reliability estimates by importance sampling. *Journal of Engineering Mechanics*, 114(12), 2195-2199. doi:10.1061/(ASCE)0733-9399(1988)114:12(2195)
- [10] Lee, I., Choi, K. K., Du, L., & Gorsich, D. (2008). Dimension reduction method for reliability-based robust design optimization. *Computers & Structures*, 86(13-14), 1550-1562. doi:http://dx.doi.org/10.1016/j.compstruc.2007.05.020
- [11] Rahman, S., & Wei, D. (2008). Design sensitivity and reliability-based structural optimization by univariate decomposition. *Structural and Multidisciplinary Optimization*, 35(3), 245-261. doi:10.1007/s00158-007-0133-3
- [12] Lee, I., Gorsich, D., Choi, K. K., Noh, Y., & Zhao, L. (2011). Sampling-based stochastic sensitivity analysis using score functions for RBDO problems with correlated random variables. *Journal of Mechanical Design*, 133(2), 021003-021003. doi:10.1115/1.4003186
- [13] Shi, L., Yang, R. J., & Zhu, P. (2012). A method for selecting surrogate models in crashworthiness optimization. *Structural and Multidisciplinary Optimization*, 46(2), 159-170. doi:10.1007/s00158-012-0760-1
- [14] Song, H., Choi, K. K., Lee, I., Zhao, L., & Lamb, D. (2011). Adaptive virtual support vector machine for the reliability analysis of high-dimensional problems. Washington, DC, USA. , 5
- [15] Zhao, L. (2011). *Reliability-based design optimization using surrogate model with assessment of confidence level*. (Ph.D., The University of Iowa). *ProQuest Dissertations and Theses*, . (894769536).
- [16] Zhao, L., Choi, K. K., & Lee, I. (2011). Metamodeling method using dynamic kriging for design optimization. *AIAA Journal*, 49(9), 2034-2046. doi:10.2514/1.J051017
- [17] Rajashekhar, M. R., & Ellingwood, B. R. (1993). A new look at the response surface approach for reliability analysis. *Structural Safety*, 12(3), 205-220. doi:http://dx.doi.org/10.1016/0167-4730(93)90003-J
- [18] An, D., & Choi, J. H. (2012). Efficient reliability analysis based on bayesian framework under input variable and metamodel uncertainties. *Structural and Multidisciplinary Optimization*, 46(4), 533-547. doi:10.1007/s00158-012-0776-6
- [19] Forrester, A. I. J., & Keane, A. J. (2009). Recent advances in surrogate-based optimization. *Progress in Aerospace Sciences*, 45(1-3), 50-79. doi:10.1016/j.paerosci.2008.11.001
- [20] Forrester, A. I. J., Sóbester, A., & Keane, A. J. (2008). *Engineering design via surrogate modelling : A practical guide*. Chichester, U.K. : J. Wiley.
- [21] Fang, H., Rais-Rohani, M., Liu, Z., & Horstemeyer, M. F. (2005). A comparative study of metamodeling methods for multiobjective crashworthiness optimization. *Computers & Structures*, 83(25-26), 2121-2136. doi:10.1016/j.compstruc.2005.02.025
- [22] Wiener, N. (1938). The homogeneous chaos. *American Journal of Mathematics*, 60(4), 897-936.
- [23] Jin, R., Chen, W., & Simpson, T. W. (2001). Comparative studies of metamodeling techniques under multiple modelling criteria. *Structural and Multidisciplinary*

- Optimization*, 23(1), 1-13. doi:10.1007/s00158-001-0160-4
- [24] Song, H., Choi, K. K., Lee, I., Zhao, L., & Lamb, D. (2011). Adaptive virtual support vector machine for the reliability analysis of high-dimensional problems. Washington, DC, USA. , 5
- [25] Agatonovic-Kustrin, S., & Beresford, R. (2000). Basic concepts of artificial neural network (ANN) modeling and its application in pharmaceutical research. *Journal of Pharmaceutical and Biomedical Analysis*, 22(5), 717-727. doi:10.1016/S0731-7085(99)00272-1
- [26] Cressie, N. A. C. (1991). *Statistics for spatial data*. New York : J. Wiley.
- [27] Sacks, J., Welch, W. J., Toby J. Mitchell, & Wynn, H. P. (1989). Design and analysis of computer experiments. *Statistical Science*, 4(4), 409-423.
- [28] Shi, L., Yang, R. J., & Zhu, P. (2012). A method for selecting surrogate models in crashworthiness optimization. *Structural and Multidisciplinary Optimization*, 46(2), 159-170. doi:10.1007/s00158-012-0760-1
- [29] Romero, D. A. (2008). *A multi-stage, multi-response bayesian methodology for surrogate modeling in engineering design*. (Ph.D., Carnegie Mellon University). *ProQuest Dissertations and Theses*, . (304667685).
- [30] Romero, D. A., Amon, C., & Finger, S. (2003). Computers and information in engineering. *Modeling Time-Dependent Systems using Multi-Stage Bayesian Surrogates*, Washington, DC, USA. 47-47-57. doi:10.1115/IMECE2003-55049
- [31] Romero, D. A., Amon, C. H., & Finger, S. (2012). Multiresponse metamodeling in simulation-based design applications. *Journal of Mechanical Design*, 134(9), 091001-091001. doi:10.1115/1.4006996
- [32] Sakata, S., Ashida, F., & Zako, M. (2007). On applying kriging-based approximate optimization to inaccurate data. *Computer Methods in Applied Mechanics and Engineering*, 196(13-16), 2055-2069. doi:http://dx.doi.org/10.1016/j.cma.2006.11.004
- [33] Sakata, S., Ashida, F., & Zako, M. (2008). Approximate structural optimization using kriging method and digital modeling technique considering noise in sampling data. *Computers & Structures*, 86(13-14), 1477-1485. doi:http://dx.doi.org/10.1016/j.compstruc.2007.05.007
- [34] Gelfand, A. E., & Smith, A. F. M. (1990). Sampling-based approaches to calculating marginal densities. *Journal of the American Statistical Association*, 85(410), 398-409. doi:10.1080/01621459.1990.10476213
- [35] Gelman, A., Carlin, J. B., Stern, H. S., & Rubin, D. B. (2004). *Bayesian data analysis*. Boca Raton, Fla. : Chapman & Hall/CRC.
- [36] Hamada, M. S., Wilson, A. G., Reese, C. S., & Martz, H. F. (2008). *Bayesian reliability [electronic resource]*. New York, NY : Springer.
- [37] Cowles, M. K. (2013). *Applied bayesian statistics [electronic resource] : With R and OpenBUGS examples*. New York, NY : Springer New York : Imprint: Springer.
- [38] Bayes, T., & Price, R. (1763). An essay towards solving a problem in the doctrine of chance. by the late rev. mr. bayes, communicated by mr. price, in a letter to john canton, A. M. F. R. S. *Philosophical Transactions of the Royal Society of London*, 53(0), 370-418.
- [39] Gilks, W. R., Richardson, S., & Spiegelhalter, D. J. (1998). *Markov chain monte carlo in practice*. Boca Raton: Boca Raton : Chapman & Hall/CRC.
- [40] Cowles, M. K., & Carlin, B. P. (1996). Markov chain monte carlo convergence diagnostics: A comparative review. *Journal of the American Statistical Association*, 91(434), 883-904.
- [41] Gelman, A., & Rubin, D. B. (1992). Inference from iterative simulation using multiple sequences. *Statistical Science*, 7(4), 457-472.
- [42] Brooks, S. P., & Gelman, A. (1998). General methods for monitoring convergence of iterative simulations. *Journal of Computational and Graphical Statistics*, 7(4), 434-455.
- [43] Song, H., Choi, K. K., Lee, I., Zhao, L., & Lamb, D. (2011). Adaptive virtual support vector machine for the reliability analysis of high-dimensional problems. Washington, DC, USA. , 5
- [44] Hastings, W. K. (1974). Monte Carlo sampling methods using Markov chains and their applications. *Biometrika*, 57(1), 97-109.
- [45] Metropolis, N., Rosenbluth, A. W., Rosenbluth, M. N., Teller, A. H., & Teller, E. (1953). Equation of state calculations by fast computing machines. *The Journal of Chemical Physics*, 21(6), 1087-1092. DOI:http://dx.doi.org/10.1063/1.1699114.
- [46] Volpi, S., Diez, M., Gaul, N. J., Song, H., Lemma, U., Choi, K.K., Campana, E.F., Stern, F. (2014). Development and validation of a dynamic metamodel based on stochastic radial basis functions and uncertainty quantification. *Structural and Multidisciplinary Optimization*, DOI: 10.1007/s00158-014-1128-5.
- [47] Sen, O., Davis, S., Jacobs, G., Udaykumar, H. S. (2015). Evaluation of convergence behavior of metamodeling techniques for bridging scales in multi-scale multimaterial simulation. *Journal of Computational Physics*, DOI: http://dx.doi.org/10.1016/j.jcp.2015.03.043.
- [48] Lee, I., Choi, K. K., and Zhao, L., (2011). Sampling-based RBDO using the stochastic sensitivity analysis and dynamic Kriging method. *Structural and Multidisciplinary Optimization*, 24, 299-317.
- [49] RecurDyn (Version 8.1) [Software]. (2000). FunctionBay, Inc. http://www.functionbay.org